

Automatic Brain Extraction of Head CT Images using Established Neuroimaging Software

John Muschelli, Natalie Ullman, Ciprian Crainiceanu

July 19, 2014

1 Introduction

X-ray computed tomography (CT) scanning is widely available and is a commonly used diagnostic tool in clinical settings [5]. Though much analysis of CT images are done by qualitative visual inspection, detailed quantification of information is of interest. CT scans do not discriminate in the tissues or structures captured; scans have non-brain structures such as the skull, eyes, facial and nasal features, extracranial skin, and more importantly non-human elements captured by the scanner, such as pillows or medical devices. These objects present a problem for extracting metrics on brain tissue. We propose a validated automated solution to brain extraction in head CT scans using established neuroimaging software.

In magnetic resonance imaging (MRI), brain extraction has been extensively studied and investigated (CITATIONS). As such, many pieces of software and algorithms exist to achieve this goal with respect to MRI scans. We have adapted one algorithm, the Brain Extraction Tool (BET) [6], a function of the FSL [1] neuroimaging software (v5.0.4), to automatically extract the brain from a CT scan. Variations of this pipeline have been presented before in Solomon et al. [7], and has been replicated in slightly more detail in Rorden et al. [4]. Neither presented a formal validation against a set of manually segmented brain images, which is the goal of our study.

2 Methods

2.1 Participants and CT data

We used CT images patients enrolled in the MISTIE (Minimally Invasive Surgery plus recombinant-tissue plasminogen activator (rtPA) for Intracerebral Evacuation) and ICES (Intraoperative CT-Guided Endoscopic Surgery) trials. These patients had an intracranial hemorrhage at time of scanning; for inclusion criteria, see Mould et al. [2]. CT data were collected as part of the Johns Hopkins Medicine IRB-approved MISTIE research studies with written consent from participants.

2.2 Imaging Data

The study protocol was executed with minor, but important, differences across the Sexprn.ctr sites. Slice thickness of the image varied within the scan for Sexprn.var.slice scans, referred to as variable slice thickness. For example, a scan may have 10 millimeter (mm) slices at the top and bottom of the brain but with 5mm slices in the middle of the brain. Therefore, the scans analyzed had different voxel (volume element) dimensions and image resolution prior to registration to the template. These conditions represent how scans are presented for evaluation in many diagnostic cases.

2.3 Manual and Automated Brain Extraction

We analyzed Sexprnscans scans, corresponding to Sexprnpt unique patients. Brain tissue was manually segmented as a binary mark from DICOM (Digital Imaging and Communications in Medicine) images in the OsiriX imaging software (OsiriX v. 4.1, Pixmeo; Geneva, Switzerland) by one expert reader (NU). CT brain

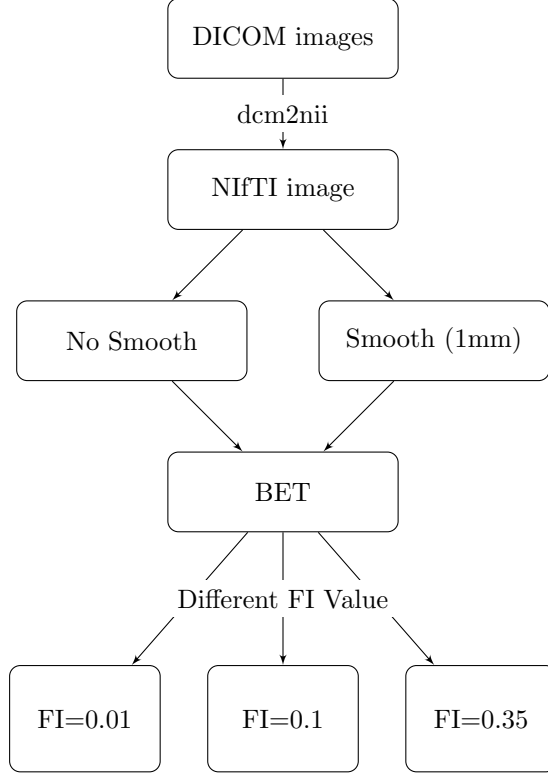


Figure 1: Overall workflow of processing of data. After the raw data has been processed and areas have been extracted, surfaces can be rendered. We are concerned with those steps in orange: creating surfaces, and export to the web. The last branch shows 2 options for export: publishing the figure to the web or enclosing it in a folder with all tools to render it. The second option would allow users to include these zipped directories as supplementary figures until more widely used.

images and the binary mask were exported from OsiriX to DICOM format. Images with gantry tilt were corrected using a customized MATLAB (The Mathworks, Natick, Massachusetts, USA) user-written script (<http://bit.ly/1ltIM8c>). Images were converted to the Neuroimaging Informatics Technology Initiative (NIfTI) data format using `dcm2nii` (2009 version, provided with MRICro [3]). Images were constrained to values -1024 and 3071 HU to remove potential image rescaling errors and artifacts. No interpolation was done for images with a variable slice thickness. Thickness was determined from the first slice converted and was assumed homogeneous throughout the image. The image processing pipeline can be seen in Figure 1.

Images were thresholded to a brain tissue range (0-100 HU). We either applied BET to the this image or smoothed this image with a Gaussian kernel ($\sigma = 1\text{mm}$, using FSL), re-thresholded to 0-100 HU and then applied BET. When BET was applied, we varied fractional intensity (FI) parameter to determine its influence on performance: we used values of 0.35 (as recommended in Rorden et al. [4]), 0.1, 0.01.

We also present one example case which demonstrates that brain extraction performance was acceptable only after smoothing before BET was applied.

2.4 Metrics of Brain Extraction Performance

Five common measurements of performance were calculated for each image: sensitivity, specificity, accuracy, Dice coefficient, and Jaccard index. Let I_{ia}, I_{im} be the indicators that voxel i for the automatic and manual masks, respectively, such that $I_i = 1$ if voxel i is labeled in the brain mask and 0 otherwise.

A true positive (TP) is defined when: $I_{ia} = 1$ and $I_{im} = 1$, a false positive (FP): $I_{ia} = 1$ and $I_{im} = 0$, a false negative (FN): $I_{ia} = 0$ and $I_{im} = 1$, and a true negative (TN): $I_{ia} = 0$ and $I_{im} = 0$. Sensitivity is

defined as

$$\frac{\#TP}{\#TP + \#FN} = \frac{\sum_{i=1}^V (I_{ia} \times I_{im})}{\sum_{i=1}^V I_{im}}$$

and specificity is defined as

$$\frac{\#TN}{\#TN + \#FP} = \frac{\sum_{i=1}^V ((1 - I_{ia}) \times (1 - I_{im}))}{\sum_{i=1}^V (1 - I_{im})}$$

and overall accuracy is:

$$\frac{\#TN + \#TP}{\#TN + \#FN + \#TP + \#FP} = \frac{\sum_{i=1}^V (I_{ia} \times I_{im}) + ((1 - I_{ia}) \times (1 - I_{im}))}{\sum_{i=1}^V I_{ia} + \sum_{i=1}^V I_{im}}$$

The Dice index is defined as:

$$\frac{2 \times \#TP}{\#TN + \#FN + \#TP + \#FP} = \frac{2 \times \sum_{i=1}^V (I_{ia} \times I_{im})}{\sum_{i=1}^V I_{ia} + \sum_{i=1}^V I_{im}}$$

3 Results

Figure 2B illustrates the performance of each variation of the BET pipeline in Figure 1. The smoothed pipelines perform better than the unsmoothed pipelines. Figure 2A displays the performance for brain extraction in the smoothed pipelines (note the change in the y-axis). Overall, using an FI of 0.35 performs worse overall than 0.01 or 0.1 for all measures other than specificity. Using an FI of 0.01 performs better than 0.1 and 0.35, although all FI perform well (above 0.95 on all measures). Therefore, smoothing with an FI of 0.01 is our recommended pipeline for CT brain extraction.

Although Figure 2 displays that using FI of 0.01 or 0.1 provides adequate results of brain extraction for most cases, they perform relatively well regardless of smoothing the data. Figure 3 displays an example where using unsmoothed data performs poorly for these FI, demonstrating why smoothing is essential for a general brain extraction procedure for CT.

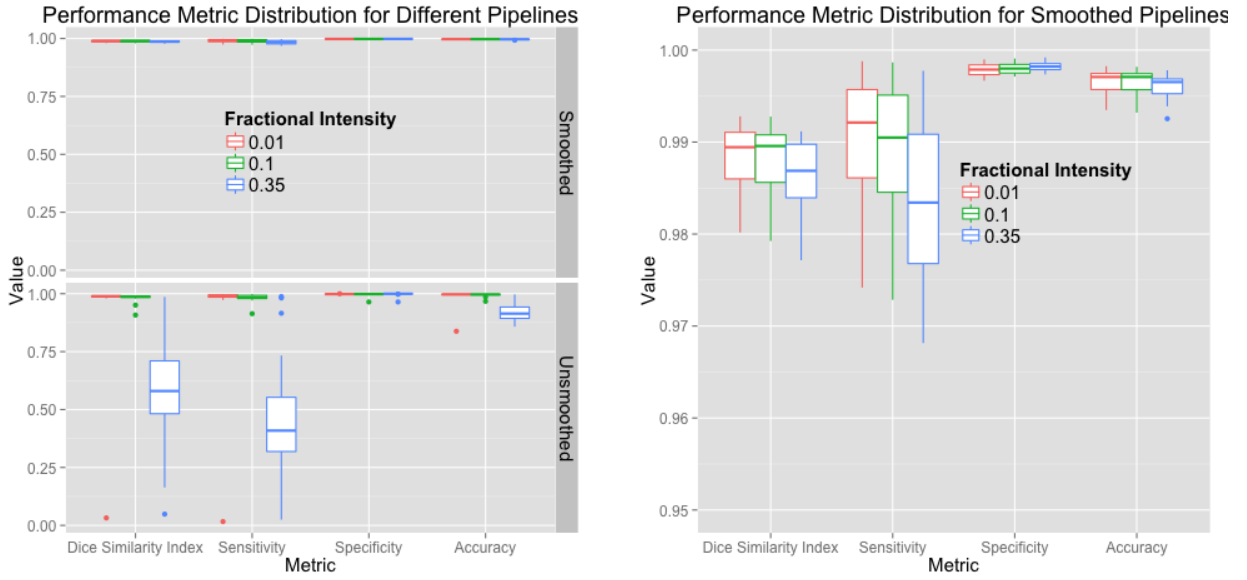


Figure 2: **Performance Metric Distribution for Different Pipelines.** Panel A displays the boxplots for performance measures when running the pipeline with a different fractional intensity (FI), using smoothed data (top) or unsmoothed data (bottom). Panel B presents the smoothed data only, rescaled to show discrimination between the different FI. Overall, FI of 0.01 and 0.1 perform better than 0.35 in all categories other than specificity. Using smoothed data improves performance in all performance metrics, markedly when an FI of 0.35 is used. Panel B demonstrates that using an FI of 0.01 on smoothed data is the best pipeline.

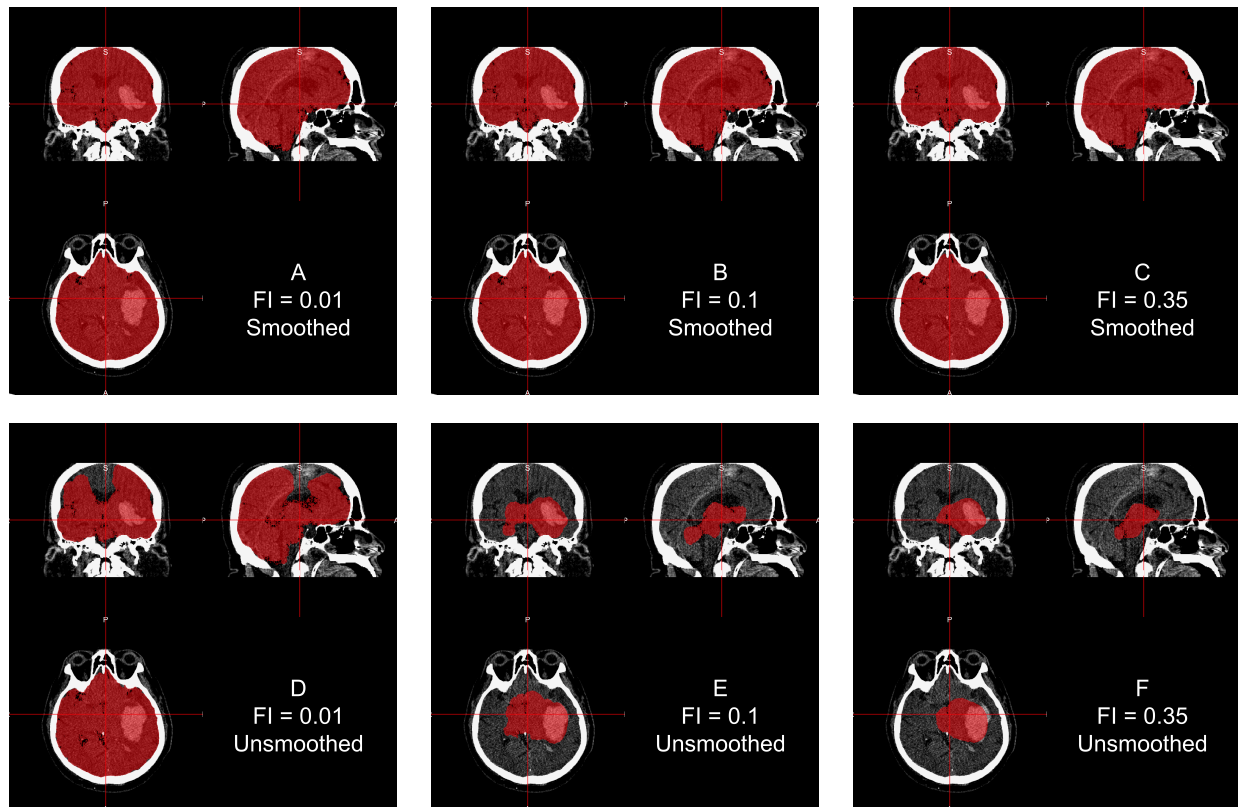


Figure 3: Example Demonstrating How Smoothing Prior to BET is Essential For one subject, the CT image is displayed with the brain extracted mask in red after running all pipelines. Panels A, B, and C represent applying BET using FI of 0.01, 0.01, and 0.35, respectively, to smoothed data. Panels D, E, and F correspond to applying BET using FI 0.01, 0.01, and 0.35 on unsmoothed data. Using smoothed data is required for adequate brain extraction.

References

- [1] Mark Jenkinson et al. “FSL”. In: *NeuroImage* 62.2 (Aug. 15, 2012), pp. 782–790.
- [2] W. Andrew Mould et al. “Minimally Invasive Surgery Plus Recombinant Tissue-type Plasminogen Activator for Intracerebral Hemorrhage Evacuation Decreases Perihematomal Edema”. In: *Stroke* 44.3 (Mar. 1, 2013), pp. 627–634.
- [3] Chris Rorden and Matthew Brett. “Stereotaxic Display of Brain Lesions”. In: *Behavioural Neurology* 12.4 (2000), pp. 191–200.
- [4] Christopher Rorden et al. “Age-specific CT and MRI templates for spatial normalization”. In: *NeuroImage* 61.4 (July 16, 2012), pp. 957–965.
- [5] Ramandeep Sahni and Jesse Weinberger. “Management of intracerebral hemorrhage”. In: *Vascular Health and Risk Management* 3.5 (Oct. 2007), pp. 701–709.
- [6] Stephen M. Smith. “Fast robust automated brain extraction”. In: *Human Brain Mapping* 17.3 (2002), 143155.
- [7] Jeffrey Solomon et al. “User-friendly software for the analysis of brain lesions (ABLE)”. In: *Computer methods and programs in biomedicine* 86.3 (2007), pp. 245–254.